KSME Journal, Vol.5, No.2, pp. 115~124, 1991

STRESS ANALYSIS AND DESIGN FOR A STRUCTURAL FATIGUE TESTING MACHINE

Soon-Bok Lee*

(Received May 2, 1991)

A closed loop servo-hydraulic structural fatigue testing machine was developed. It can apply fatigue loads on actual engineering parts or components for their fatigue strength evaluation. The testing machine consists of a structural bending load frame, a structural torsion load frame, a hydraulic system, and a control system. Stress analysis and design for the crosshead, columns, and test bed for the structural bending test frame are described. Finite element analysis was performed for the structural torsion load frame. Evaluation of the structural load frames and application of the test machine are briefly given.

Key Words: Design, Structural Fatigue Testing, Stress Analysis, Strength Evaluation, Synthesis, Testing Machine

NOMENCLATURE

f : Material fringe value
m : number of cylinders
n : Number of columns
P_h : Hydraulic pressure in the clamping cylinder
B : Thickness of the crosshead
D_c : Inner diameter of clamping cyclinder
D_r : Diameter of rod
E : Young's modulus
F : Force exerted by clamping cylinders
I_{zz} : Second moment of inertia about z-axis
L : Length of the column.
M_{max} : Maximum bending moment
N : Fringe order
P : Maximum force exerted by the acutator
P_θ : Pressure distribution on the clamping surface
R : Radius of column
T : Thickness of the clamping part defined in Fig. 5(c)
T_{max} : Maximum distance from the bending axis
V_θ : Vertical force at angle θ induced by F
U : Strain energy of the clamping part by moment and forces acting on it
W : Weight of the corsshead
δ_θ : Vertical deflection at angle θ
σ_B : Buckling stress
σ_c : Compressive strength of the material
μ : Friction coefficient between crosshead and column
ν : Poisson's ratio

Subscripts

p : Prototype
m : Model

1. INTRODUCTION

Structural fatigue tests are often required in engineering practice, owing to the shortcomings of relating material behavior with structural behavior and the lack of accuracy in knowing the loads in individual structural elements. The main advantage of structural testing is well known to be its capability to find out all the weak spots in the total design, and thereby to show where and when to inspect the structure in service. For structural fatigue tests, the proper testing machine is essential. Yet, structural fatigue testing machines are not as readily available as material fatigue testing machines. Therefore, we have developed a versatile structural fatigue testing machine utilizing a closed loop hydraulic servo system. The testing machine consists of load frames, a hydraulic system, and a control system.

The load frames, as shown in Fig. 1, consist of two

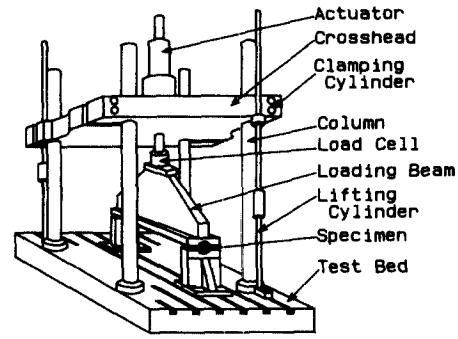

(a) Structural Bending Load Frame

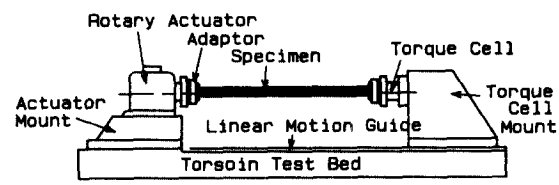

(b) Structural Torsion Load Frame

Fig. 1 Schematic configuration of the load frames for the structural fatigue testing machine.

*Department of Mechanical Engineering, Korea Advanced Institute of Science and Technology, Taejon 305-701, Korea

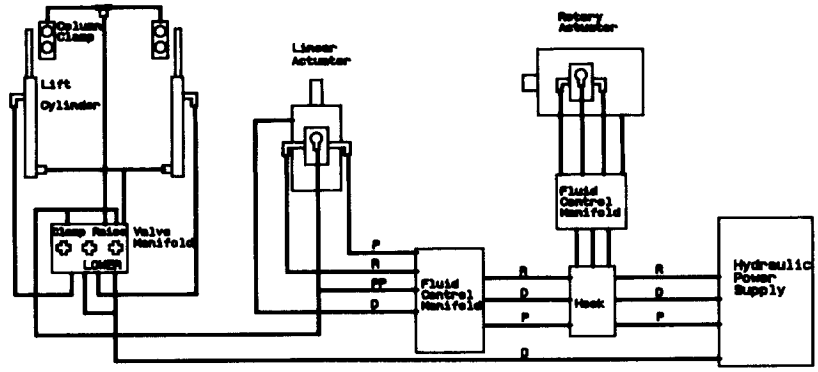

Fig. 2 Hydraulic system for the structural fatigue testing system. (P indicates pressure line, R indicates return line, D indicates drain line, and PP indicates pilot pressure)

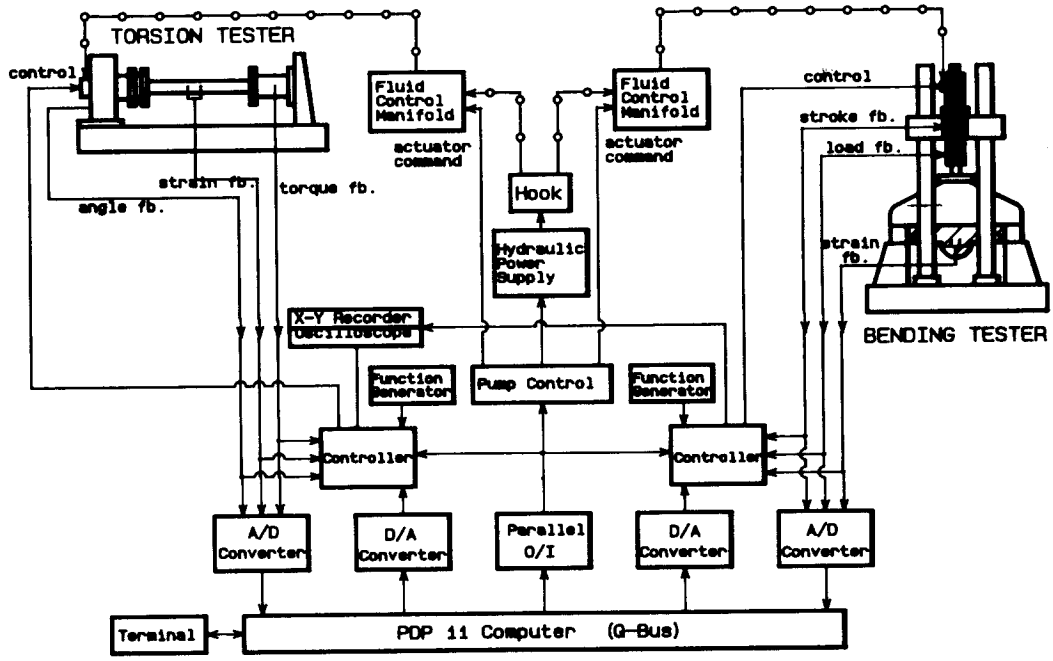

Fig. 3 Block diagram of the control system for the fatigue testing machine.

frames : a structural bending load frame and a structural torsion load frame. The bending load frame was made on the basis of our design, whereas the torsion load frame was merely constructed by utilizing an available bed. For the design, we performed stress analysis both theoretically and experimentally, which will be extensively discussed. To check the adequacy of the available bed, on the other hand, we performed finite element analysis.

The hydraulic system for the structural fatigue testing machine is schematically shown in Fig. 2. It consists of one hydraulic power supply and four hydraulic circuits : a linear actuator circuit, a rotary actuator circuit, a lifting circuit, and a clamping circuit for the crosshead of the bending load frame. The hydraulic power supply provides 20 GPM of flow rate with 20.6 MPa of pressure on the system. Among the hydraulic circuits, the lifting circuit was used to adjust the testing space by lifting or lowering the corsshead, and the clamping circuit to exert necessary clamping forces after the testing space adjustment. Two lifting cylinders were designed and used in the lifting circuit ; the clamping cylinders in the clamping circuit.

The control system, as described in the block diagram in Fig. 3, consists of controllers, function generators and data acquisition system. For the data acquisition and control the fatigue testing, A/D and D/A converters, and a Micro PDP-11 computer were used.

Overall specification of the system is given in Table 1.

Table 1 Specification of the structural fatigue testing machine

	Bending Testing	Torsion Testing
Max. Dynamic Load	±490kN	±20kN·m
Max. Displacement	150mm	±50degree
Max. Specimen Size	7500×1500×950mm	2500mm
Max. Test Frequency	20Hz.	15Hz
Control Mode	Load, Stroke, Strain	Torque, Angle, Strain

2. STRESS ANALYSIS AND DESIGN FOR THE BENDING LOAD FRAME

In designing the fatigue testing machine, we considered that all frame parts are required to be durable and capable of transmitting the necessary forces and performing the necessary motions efficiently and economically without interfering with any other part of the machine.

In the conceptual design stage, several shapes of the bending load frame were considered. Among the shapes considered, a column type load frame was chosen rather than a welded type load frame in order to guarantee versatility in applications. In actual design of the chosen frame, stress analysis was performed based on the "safe-life" design philosophy by Fuchs and Stephens(1980). Fig. 1 (a) shows the resulting schematic configuration of the structural bending load frame.

The structural bending load frame has four columns, a test bed and a crosshead. On the crosshead a 490 kN linear actuator is installed in an upside down position, with one end of the acutator rod connected to a load cell. Under the load cell a bending loading beam is attached to apply four point bending loads on a structural specimen such as an axle housing. To accommodate the various specimen size, inverse T-shape slots are made on the test bed. On the test bed four columns stand, and on the columns a crosshead is clamped with eight hydraulic clamping cylinders, two on each column. In the following subsections, we will present the stress analysis to determine the dimensions and design procedures of the crosshead, the column, the test bed and its foundation.

2.1 Crosshead Design.

The most difficult part of the design of the structural fatigue testing machine was the design of the crosshead. It required the careful stress analysis and synthesis for the stiffness, geometric compatibility, manufacturability, and clamping force exerted by the crosshead on columns. The clamping part is subjected to a fatigue load under repeated clamping actions. The excessively conservative design against fatigue loading may require unnecessary high clamping force and as the consequence the fretting failure may occur in the clamping surface contacting the columns. Among several plausible shapes of crosshead considered in the conceptual design stage, the shape shown in Fig. 1 (a) was determined because it has the simple manufacturing process and relatively smooth stress distribution around the clamping part.

The width and length of the crosshead were determined to be 880 mm and 1540 mm, in order to ensure geometric compatibility with the testing space and clamping cylinders. To obtain the proper thickness, deflections of the corsshead were calculated under 500 kN and 1000 kN loads at various thicknesses as shown in Fig. 4. The crosshead thickness was determined to be 300 mm by using the maximum allowable deflection of the crosshead as 0.05 mm for a stiffness requirement.

The stress analysis for the crosshead design was essential to optimize the dimension of the clamping part, so that it would easily deflect for the low clamping force requirement yet have low stress during the clamping action to avoid the fatigue failure. In the current design the crosshead can be clamped on columns if the following condition is satisfied

$$2\mu B\int_0^{\pi} P_\theta R d\theta \geq (P+W)/n \tag{1}$$

where μ is the friction coefficient between crosshead and column, B is the thickness of the crosshead, P_θ is the pressure distribution on the clamping surface, R is the radius of column, P is the maximum force exerted by the actuator, W is the weight of the crosshead and n is the number of columns.

To find the P_θ, a schematic and simplified model for a parametric stress analysis for the design of the clamping part as shown in Fig. 5(a) was considered. The force equilibrium

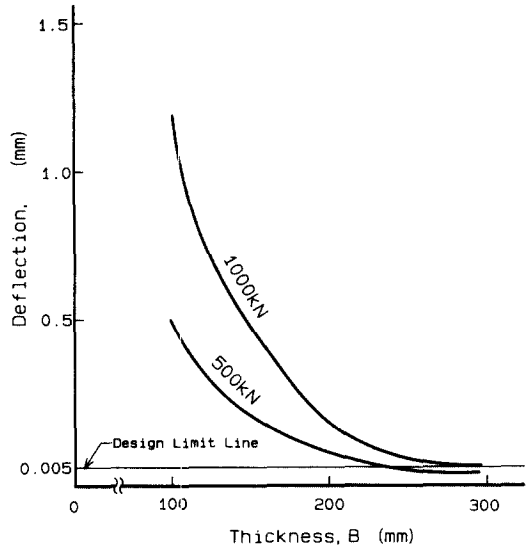

Fig. 4 Crosshead deflection versus crosshead thickness at 500kN and 1000kN.

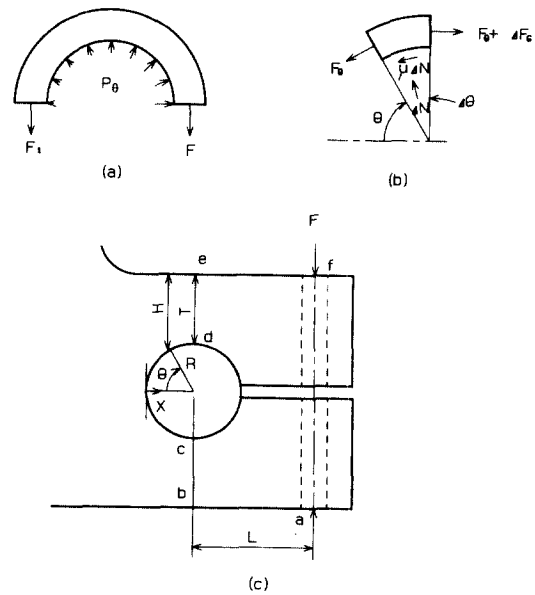

Fig. 5 Free body diagram and geometry of the clamping part ; (a) a schematic and simplified model for a parametric stress analysis, (b) free body diagram of a clamping element and (c) geometry and definitions, a, b, c, d, e, f are locations where photoelastic stress analysis were performed.

of the free body diagram provides

$$F+F_1=\int_0^{\pi} P_\theta \cdot B \cdot R \cdot \sin\theta \cdot d\theta \tag{2}$$

where F is the force exerted by clamping cylinders and defined as

$$F=\frac{\pi}{4}\cdot(D_c^2-D_r^2)\cdot p_h \cdot m \tag{3}$$

where D_c is inner diameter of clamping cylinder and, D_r is diameter of rod, p_h is the hydraulic pressure in the clamping cylinder, m is the number of cylinder. To find the force F_1, F_θ at angle θ was obtained from the force equilibrium of the clamping element shown in the Fig. 5(b) with following relation

$$\frac{dF_\theta}{F_\theta}=\mu\cdot d\theta \tag{4}$$

By integrating the Eq. (4) with the boundary condition of $F_\theta=F$ at $\theta=\pi$, the F_θ becomes

$$F_\theta=F\cdot e^{\mu(\theta-\pi)} \tag{5}$$

and F_1 at $\theta=0$ becomes

$$F_1=F\cdot e^{-\mu\pi} \tag{5}$$

The clamping cylinder was designed to satisfy the clamping condition defined in Eq. (1) with the P_θ obtained by the following analysis.

The actual P_θ distribution can be considered as the superposition of a uniformly distributed function and a nonuniformly distributed function. If P_θ is a uniformly distributed function only, from Eq. (2) P_θ becomes

$$P_\theta=\frac{F+F_1}{2\cdot B\cdot R} \tag{6}$$

If P_θ is now a nonuniformly distributed function only, the shape of P_θ distribution can be similar to the deflection curve of the clamping part without column. The deflection curve δ_θ then was calculated according to the Castigliano's theorem explained by Boresi et al.(1978) using the following equation

$$\delta_\theta=\frac{\partial U}{\partial V_\theta} \tag{7}$$

where δ_θ is the vertical deflection at angle θ, V_θ is the vertical force at angle θ induced by the clamping force F, and U is the strain energy of the clamping part by moment and forces acting on it. The deflection curve of the clamping part was calculated according to the Eq. (7) and shown in Fig. 6. Then, the nonuniform distribution P_θ can be related with δ_θ as

$$P_\theta=\frac{\delta_\theta\cdot F}{A\cdot B} \tag{8}$$

where A is the slashed area in Fig. 6, and B is the thickness of the crosshead.

The stress analysis for design based on Fig. 5(a) and (b)

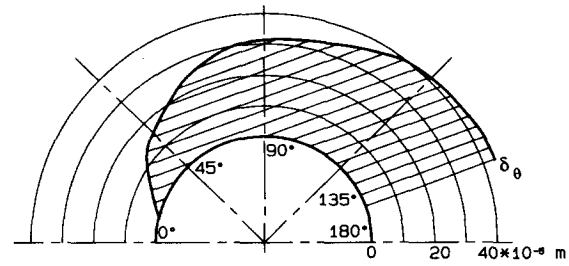

Fig. 6 A curve of the vertical deflection of the clamping surface at arbitrary angle θ.

provided the parametric information in the clamping part design. For the manufacturability of the crosshead which requires the precision machining on a relatively large piece of heavy steel casting, the clamping part of the crosshead was decided as shown in Fig. 5(c). The thickness T at the clamping part has to be optimized to have more structural reliability and less clamping force. The maximum bending stress and shear stress of the clamping part depend on the thickness T as

$$\begin{aligned}\sigma_{x,max}&=\frac{F\cdot(L+R-X)\cdot\frac{H}{2}}{B\cdot H^3/12}\\ \tau&=\frac{F}{B\cdot H}\\ H&=R+T-\sqrt{R^2-(R-X)^2}\end{aligned} \tag{9}$$

where H, L, R, X are defined in Fig. 5 (c).

Since the clamping force and the thickness of the clamping part are related and their plausible values can be obtained by iteration, a computer program was developed based on the above simple Eqs. (1~9) and the final geometry shown in Fig. 5(c) to calculate the clamping force and optimal dimensions around the clamping part in the crosshead. Fig. 7 shows

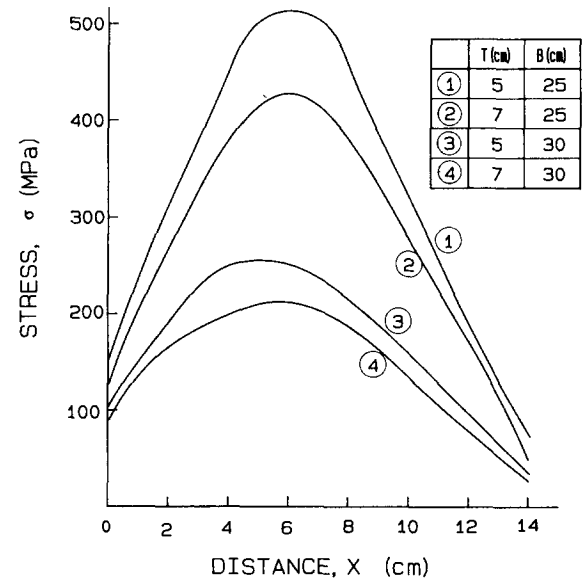

Fig. 7 Stress distribution along the distance X at the clamping part. T is the thickness of the clamping part defined in Fig.5(c) and B is the thickness of the corsshead.

Table 2 Stress simulated by a photoelastic method

measured points	a	b	c	d	e	f	
fringe order	1.83	2.72	2.88	2.70	2.9	1.83	Tardy method
σ_m(MPa)	1.95	2.9	3.07	2.88	3.09	1.95	F_m=4.9kN
σ_p(MPa)	99.5	147.9	156.6	146.8	157.7	99.5	F_p=250kN

the maximum combined stress distribution along the distance X of the clamping part.

As a part of the synthesis, a photoelastic stress analysis with a reflection polariscope system was performed on the points shown in Fig. 5 (c) to experimentally check the adequacy of the design because the final design configuration is somewhat different from the simplified model for the stress analysis. The strain and the photoelastic fringe is related as $\varepsilon_x-\varepsilon_y=f\cdot N$ according to Zandman and Redner and Daly (1977). Since maximum stress occurs at the surface in the model, the stress can be expressed as

$$\sigma=f\cdot N\cdot\frac{E}{1+\nu} \tag{10}$$

where f is the material fringe value, N is the fringe order, ν is Poisson's ratio. A small one tenth model was made with photoelastic coating material, type PS-1A whose properties are ; E=2480 MPa, $\nu=0.38$, $f=593\times10^{-6}$, $t=3$ mm. The stress in the prototype can be related with the stress in the model as

$$\sigma_p=\sigma_m\cdot\frac{F_p}{F_m}\cdot\left(\frac{L_m}{L_p}\right)^3 \tag{11}$$

where F is force, L is length ; and the subscripts, p and m, denote prototype and model respectively. Table 2 shows the experimental stress analysis results by the photoelastic method. The maximum stress occurred at point e in the photoelastic model and the maximum stress in the prototype was 157.7 MPa when the clamping force was 250kN. Since the yield strength and tensile strength of the crosshead material SC46C cast steel are 225.4 MPA, 450.8 MPa respectively, the maximum stress in the prototype guarantees the safe life under structural fatigue testing.

In addition, fretting fatigue failure may occur on the crosshead at the clamping area contacts with the columns. To avoid such fretting fatigue, aluminium bushings were inserted between the columns and the crosshead. It is common practice to use bushings for reducing friction, but rare to use for avoiding fretting fatigue.

2.2 Column Design

Columns should be safe from yielding and buckling, and should satisfy the stiffness requirement. Yielding can be prevented if the column diameter, D, satisfies the following condition

$$D^2\geq\frac{4\cdot P\cdot S_f}{\pi\cdot n\cdot\sigma_y} \tag{12}$$

where P is the maximum fatigue load, S_f is safety factor, σ_y is yield stress, n is the number of column.

Buckling stress was calculated according to Rankine's formula

$$\sigma_B=\frac{\sigma_c}{1+\frac{1}{1500}\left(\frac{4L}{D}\right)^2} \tag{13}$$

where σ_B is buckling stress, σ_c is compressive strength of the material, and L is the length of the column.

The spring rate of the column for the material fatigue testing machine is known to be about 32.7×10^8 N/m, which corresponds to 0.15 mm deflection under 490 kN load. The deflection δ was calculated as

$$\delta=\frac{4\cdot P\cdot L}{n\cdot\pi\cdot D^2\cdot E} \tag{14}$$

where E is Young's modulus of the column material. The material properties for the SF55A steel used in the columns were σ_y=275 MPa and E=215 GPa. Fig. 8 shows the feasible region of column diameter with 0.1mm deflection limit. By satisfying the stiffness requirement with 132 mm in diameter and 2500 mm in length, the safety factors in column design were around 15 for yielding and 5 for buckling.

The frame of the structural fatigue testing machine is subjected to fatigue loading. Figure 9 shows the various methods of joining the columns on the bed, among which method (a) is relatively easy to assemble and good for fatigue loading. In designing the column step, the shear stress and the stress concentration must be considered. The step height h can be expressed as

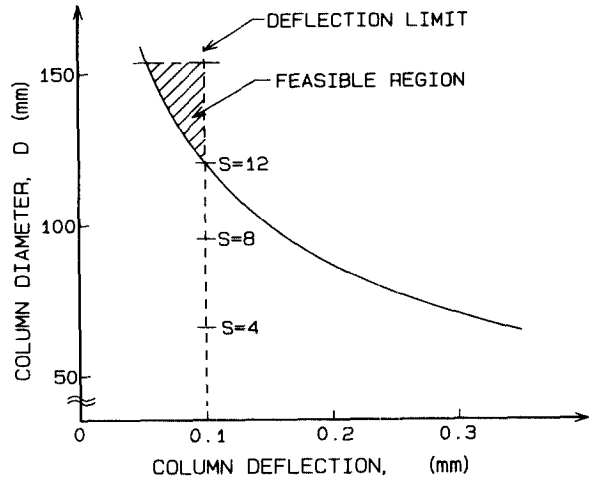

Fig. 8 Feasible region of column diameter with 0.1mm deflection limit.

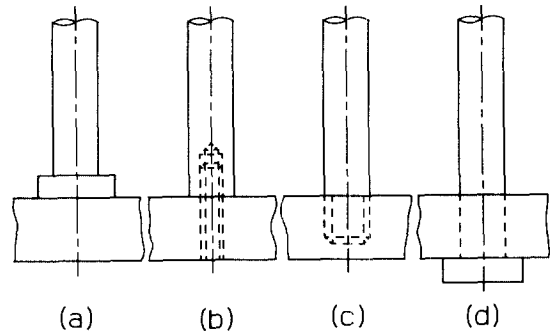

Fig. 9 Various methods of joining the columns on the bed.

$$h=\frac{P\cdot S_f}{n\cdot\pi\cdot D\cdot\tau} \tag{15}$$

where τ is the allowable shear stress of the column material and D is the column diameter. The step height was determined to be 100 mm and the step diameter to be 220 mm to adapt to the bolt holes. Twelve M20 bolts were used for joining the each column on the bed by considering the fatigue loading.

Since the column and the step must be made from one piece, the manufacturing process of the column with the step was forging, machining, and then hard chrome plating for enhancing the surface wear resistance and hardness.

2.3 Test Bed and Foundation Design

(1) Test bed design

The test bed was designed with constraints of bending stress and deflection to adapt various types of rigs for structural bending fatigue tests. The maximum allowable stress and deflection were determined to be 50 MPa and 0.4 mm respectively. For the stress analysis, the deflection function $\delta(x)$ of the test bed can be assumed as

$$\delta(x)=a\cdot\delta_1(x)+b\cdot\delta_2(x)+c\cdot\delta_3(x) \tag{16}$$

where a, b, c are constants, $\delta_1(x)$ is deflection function of simply supported beam, $\delta_2(x)$ is deflection function of fixed beam of two ends, and $\delta_3(x)$ is deflection function by weight.

The maximum bending stress of the beam can be expressed as

$$\sigma_{max}=\frac{M_{max}\cdot T_{max}}{I_{zz}} \tag{17}$$

where M_{max} is maximum bending moment, T_{max} is the maximum distance from the bending axis, and I_{zz} is the second moment of inertia about z-axis. Among various types of test bed considered during the conceptual design stage, rib type test bed was chosen, having a high second moment of inertia with low weight. It is shown in Fig. 10. The length and width of the test bed were determined to be 2300 mm and 1400 mm to be made compatible with testing space and column stands. To calculate the bending stress and deflection of the test bed shown in Fig. 10, a computer program was developed based on the Eqs.(16) and (17). The resulting deflection and bending stress versus test bed thickness calculated with the program are shown in Fig. 11. From Fig. 11, $T_1=200$ mm, $T_2=100$ mm were determined for the thickness to satisfy the constraints of bending stress and deflection of the test bed.

(2) Foundation Design

For a reliable foundation design, the expected maximum stress acting on the foundation was required. The forces acting on the foundation depend on the type of test. In a four point bending test, tension load occurs on the ancor bolt near the columns and compression load occurs on the ancor bolt

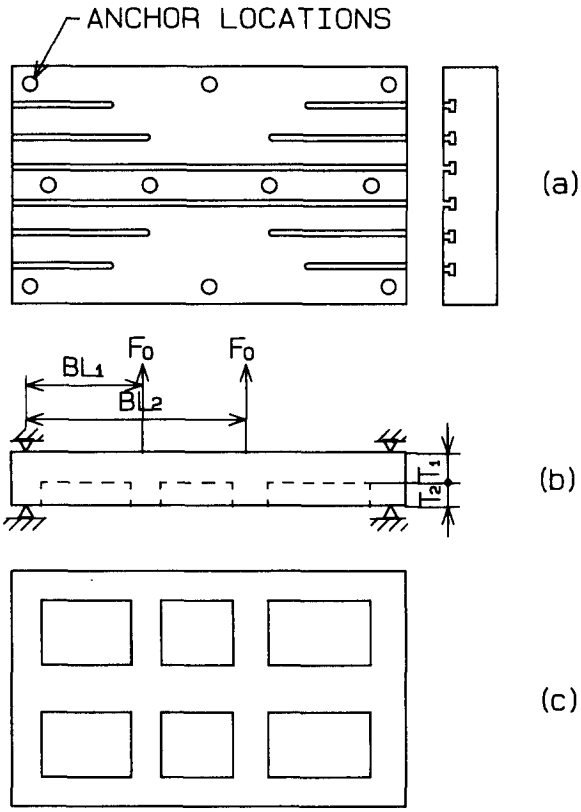

Fig. 10 Geometry of the test bed ; (a) top view, (b) side view and definition and (c) bottom view.

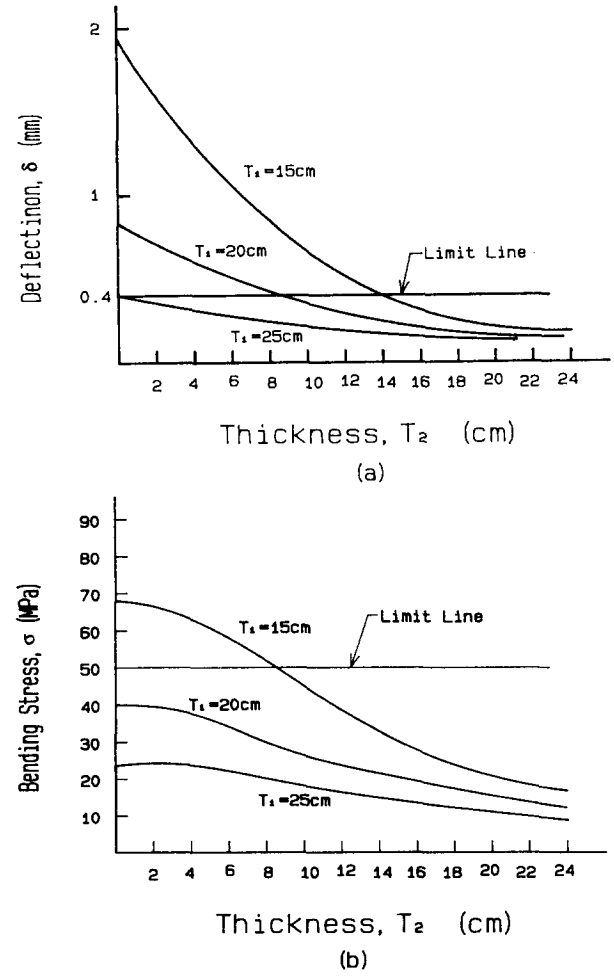

Fig. 11 Results of analysis for the design of test bed ; (a) deflection curves versus test bed thickness and (b) bending stress curves versus test bed thickness.

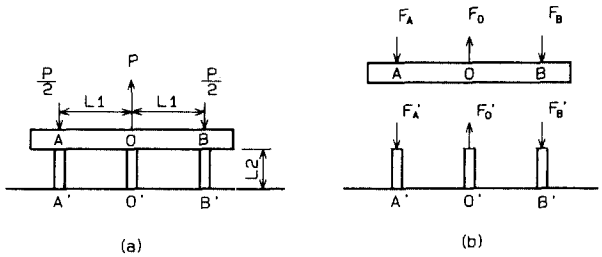

Fig. 12 Schematic illustration for the foundation design ; (a) idealized diagram of the test bed, anchor bolt, and foundation and (b) simplified free body diagram.

near the fixture. Fig. 12 shows the idealized schematic diagram of the foundation, anchor bolt, and test bed.

From the equilibrium of forces, the following relations were obtained.

$$F_A=F_B,\ F_A+F_A'=\frac{P}{2},\ F_o+F_o'=P \tag{18}$$

where F_A, F_B, F_o are the forces acting on the test bed, and F_A', F_B', F_o' are the forces acting on the anchors, and P is the maximum fatigue loading.

The deflections of the bed were obtained by assuming the clamped ends

$$\delta_A=\frac{2F_A(2L_1)^3}{192E_bI},\ \delta_o=\frac{F_o(2L_1)^3}{192E_bI} \tag{19}$$

where δ_A, δ_o are the deflections of the bed at point A, and O, and I is the second moment of inertia, E_b is the Young's modulus of the bed, L_1 is the distance from the center to the end anchor on the bed. The deflections of the bed follow by assuming the simply supported ends

$$\delta_A=\frac{F_AL_1^3}{3E_bI},\ \delta_o=\frac{F_o(2L_1)^3}{48E_bI} \tag{20}$$

The actual deflections of the bed will be between values by Eqs. (19) and (20). It is safe to use Eq. (20) for load-deflection relation because it provides the upper bound value for design criteria.

The deflections of anchor bolts are

$$\delta_A'=\frac{F_A'L_2}{AE_a},\ \delta_0'=\frac{F_o'L_2}{AE_a} \tag{21}$$

where δ_A', δ_o' are the deflections of the anchors A, and O, E_a is the Young's modulus of the anchor.

From the geometric compatibility

$$\delta_A=\delta_A',\ \delta_o=\delta_o' \tag{22}$$

From Eqs. (18), (20), (21), and (22) the forces transmitted to the anchors A and O are

$$F_A'=\frac{P}{2\cdot\left[1+\frac{3\cdot I\cdot E_b\cdot L_2}{A\cdot E_a\cdot L_1^3}\right]},\ F_o'=\frac{P}{1+\frac{6\cdot I\cdot E_b\cdot L_2}{A\cdot E_a\cdot L_1^3}} \tag{23}$$

By the numerical values, $I=2.95\times10^0$ cm^4, $A=12.57$ cm^2, $L_1=100$ cm, $L_2=17.4$ cm, $E_b/E_a\approx1$ the Eq. (23) becomes

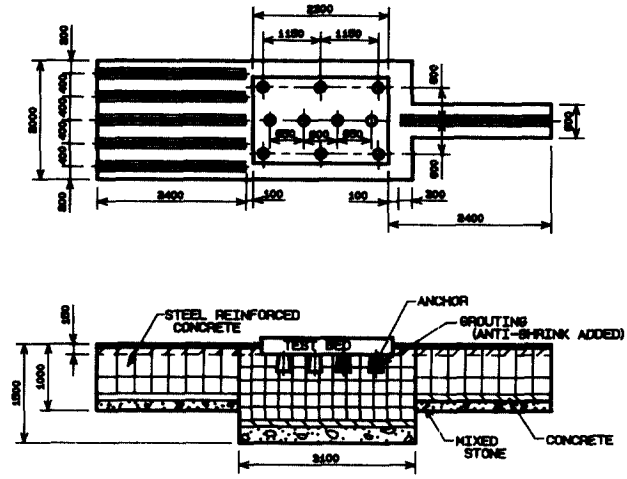

Fig. 13 The configuration of the foundation of the structural bending fatigue testing frame. (Dimensions in mm)

$$F_A'=0.23P\text{(compression)}\ \ F_o'=0.29P\text{(tension)} \tag{24}$$

By designing three compression anchors at one side and four tensile anchors at the center of the bed, a fatigue loading $P=490$ kN caused, the stresses transmitted on the foundation through the anchor base whose diameter was 14cm were calculated as 2.3 MPa tensile and 2.4 MPa compression. The concrete strength is known to be about 20 MPa in compression and 2.6 MPa in tension. Since the concrete strength was not sufficient in tension, the steel reinforced concrete was used in the foundation and grouting was performed with anti-shrink additive around the anchor boxes and beneath the grooved slabs used for the bed extension as shown in Fig. 13. The extended bed with the grooved ground slabs installed on the foundation can accommodate long structural specimens up to 7500 mm.

3. EVALUATION OF BENDING LOAD FRAME

3.1 Inspection of the Load Frame

Ultrasonic tests were performed with a 2 MHz, 24 mm diameter transducer. Internal voids and defects in the crosshead and test bed were detected : but were acceptable according to ASTM A609 and A388. No void was detected in columns. Roundness of columns, flatness of test bed and crosshead, and squareness between column and test bed were inspected because they are related with the accuracy of fatigue testing. They were all satisfactory.

3.2 Stiffness of the Load Frame

The deflection of the load frame was measured as 0.075 mm with a 300 kN load and 1520 mm of crosshead height. The deflection of the load frame was also calculated as 0.06mm, but it is slightly lower than the measured value because of the simplification of the frame in calculation. The measured spring rate of the load frame was about 40×10^8 N/m, which is sufficiently stiff for the structural fatigue testing.

3.3 Vibrational Aspect of the Load Frame

The vibrational characteristics of the frame was investigated analytically, numerically and experimentally, in order to

determine the safe region of structural fatigue festing frequencies. The significant natural frequency was found to be 120 Hz by experimental modal analysis. The maximum bending test frequency was determined to be about 20 Hz, because to avoid resonance effects the test frequency must be less than one fourth of the natural frequency of the load frame according to Tse and Morse and Hinkle(1978). The detail analysis and test procedure for the vibrational characteristics were described by Lee and Lee(1989).

Lists of computer programs developed for the stress analysis for design are reported by Lee et. al(1983).

4. ANALYSIS FOR THE TORSION LOAD FRAME

The torsion load frame shown in Fig. 1(b) consists of an actutor mount, a torque cell mount, a linear motion guide, and a test bed. To check the adequacy of the test bed for the structural torsion load frame, finite element analysis was performed. Fig. 14 shows the finite element model of the structural torsion fatigue testing frame to find its stress,

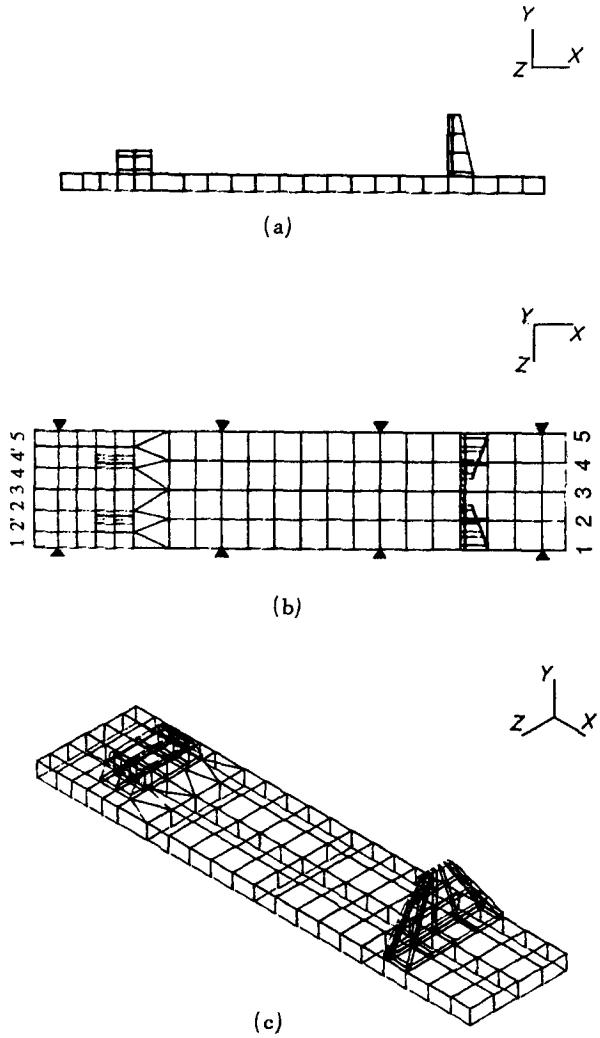

Fig. 14 Finite element model of the structural tosion fatigue testing frame ; (a) side view. (b) top view, black triangles indicate the location of bolts on foundation, and (c) overall view.

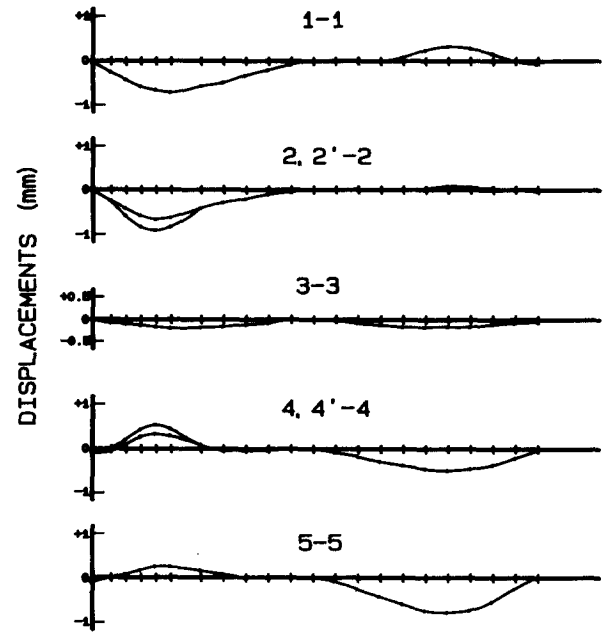

Fig. 15 Deformation curves of the torsion fatigue test bed at the maximum static load along the longitudinal lines defined in Fig. 14(b). (Vertical dimensions in mm)

deformation, and vibrational modes. From this analysis, the deformation curves of the test bed at the maximum static load were obtained and shown in Fig. 15. Maximum deflection occurred at the actuator mounting area. From this result, the total twisting angle of the frame was calculated to be 0.193 degree, which is 39% of the maximum allowable twist angle, 0.5 degree, in reliable fatigue testing. And the maximum stress 28 MPa occurred at the same location of the maximum deflection. Material of the torsion bed was GC25 cast steel whose tensile strength is 250 MPa.

The above analysis showed that the test bed was adequate for the structural tosion fatigue testing frame because it had sufficient rigidity and strength. The torsion test bed was then fixed with foundation bolts, which gave more torsional rigidity.

A 20 kN·m rotary actuator fixed on the test bed can apply the cyclic torsion load on a torsion specimen attached to the torque cell, whose mount moves on the linear motion guide. This arrangement can prevent any unwanted axial load during the structural torsion fatigue testing and also can accommodate a torsion specimen such as automobile drive shaft or torsion bar of any length up to 2500 mm.

Finite element analysis also showed the lowest natual frequency of the structural torsional fatigue testing frame was 67 Hz. The maximum torsion testing frequency was then specified to be about 15 Hz, so that the natural frequency of the frame would be at least four times higher than the test frequency to avoid resonance effects as suggested by Tse and Morse and Hinkle(1978).

5. APPLICATION OF THE STRUCTURAL FATIGUE TESTING MACHINE

5.1 Structural Bending Test of a Rear Axle Housing

A rear axle housing from a 98 kN truck was tested under

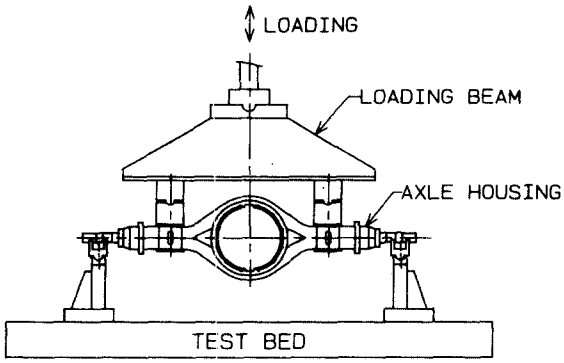

Fig. 16 Arrangement for the four point bending fatigue testing of the rear axle housing.

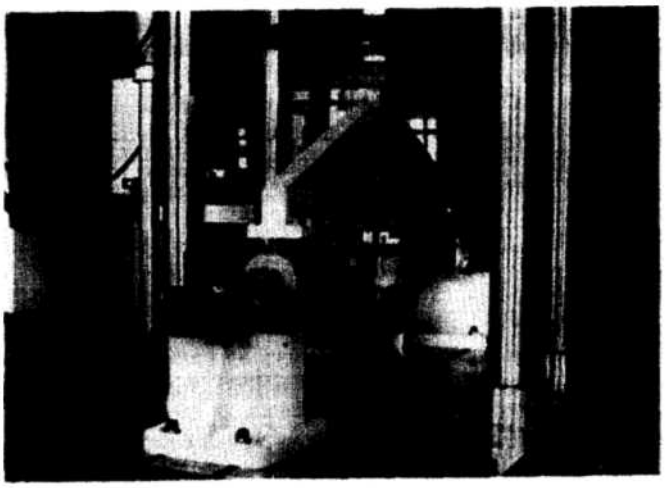

Fig. 17 Four point bending fatigue test setup for a rear axle housing with the structural fatigue testing machine developed.

four point bending fatigue loading at 2 Hz. The expected service load was 37.7 kN for the rear axle housing made of AISI1035 steel. The range of test load was 5 to 200% of the service load. Loads and deflections were monitored with the fatigue test monitoring program developed for the test automation. Cracks were detected at the heat affected zone by the weldment on the axle housing after around 300,000 cycles. Figure 16 shows the arrangement for the four point bending fatigue test of the rear axle housing. Several different types of axle housings were tested under static and cyclic step loading with the strcutural fatigue testing machine. Fig. 17 shows one of the examples of such structural fatigue testings.

5.2 Structural bending Test of a Leaf Spring

Durability of a leaf spring for a 108 kN truck was tested under three point bending fatigue loading at 0.2 Hz. The test load range was 9 kN to 200 kN and the deflection range of the leaf spring was 7 mm to 58 mm. The leaf spring endured 60,000 cycles without a failure. Fig. 18 shows the test setup for a leaf spring with the structural fatigue testing machine developed so far.

5.3 Structural Fatigue Testings of Automobile Components

Fatigue strength evaluations of automobile components

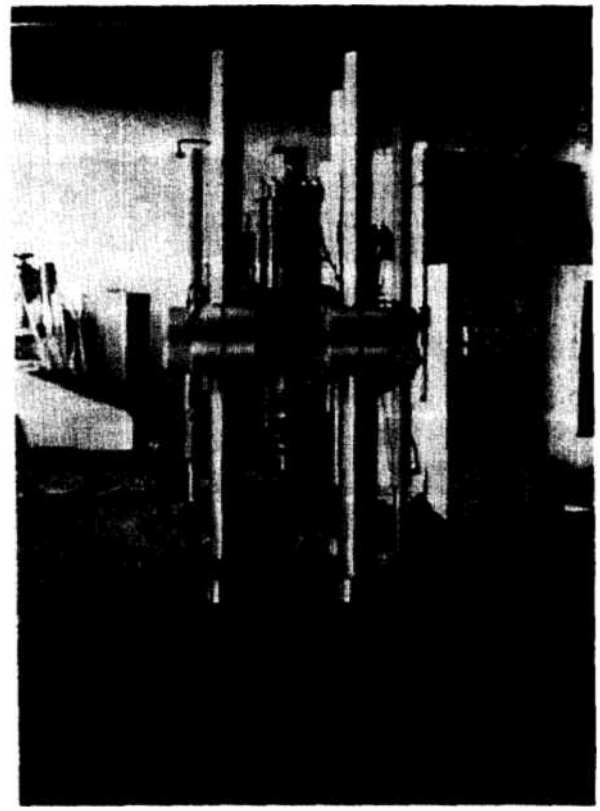

Fig. 18 Three point bending fatigue test setup for a leaf spring with the structural fatigue testing machine developed.

such as crank shafts, steering knuckles, suspension springs, and a torque rod assembly were performed successfully with various test jigs on the structural bending fatigue testing machine. The fatigue strength evaluation of the torque rod assembly with the structural fatigue testing machine promoted the industry to develop the reliable torque rod assembly with less cost. Full descriptions of the applications of the fatigue testing machine are beyond the scope of this paper. The detailed descriptions on the various examples evaluated with the fatigue testing machine were given by Lee et al. (1988). The acceptance criteria for the automobile components and test conditions with the structural fatigue testing machine were described by Lee(1985).

5.4 Structural Torsion Test

Structural fatigue tests were performed with six rear axle shafts of 24.5 kN trucks under a repeated torque of ± 4.5 kN ·m and 0.5 Hz. The dimension of the axle shaft was 987 mm long and 37 mm in diameter. Cracks occurred along the longitudinal shear plane and on the plane perpendicular to the principal tensile stress. The six specimens failed at 65000, 54800, 36000, 30400, 26000, and 41000 cycles. A Weibull plot was made with the results. The B-10 life was then found to be about 22000 cycles for the axle shaft. The Weibull slope b was 2.95 which indicates the fatigue failure is close to normal distribution according to Little and Ekvall(1979).

Fatigue strength evaluation of drive shafts, shafts with universal joint, and shaft with constant velocity joint were performed successfully with various adaptors on the structural torsion testing frame. Fig. 19 shows the torsion fatigue test setup for a driveshaft with the structural fatigue testing

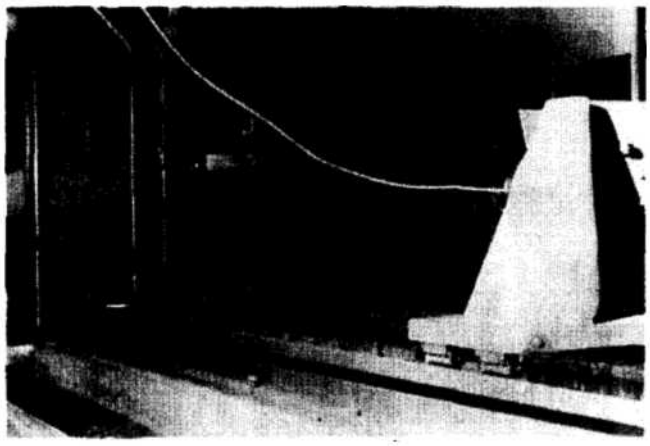

Fig. 19 Torsion fatigue test setup for a driveshaft with the structural fatigue testing machine developed.

machine developed.

6. CONCLUSION

A closed loop servo-hydraulic fatigue testing machine was designed and developed. Detailed stress analysis was performed for the bending frame design. Stress analysis and synthesis with a simple analytical model and photoelastic means were performed to confirm dimensional adequacy of the crosshead under several constraints such as stiffness, geometric compatibility, and clamping force exerted by the crosshead on columns. The bending load frame was thoroughly inspected and critically evaluated for the accuracy of testing and it was found suitable for various structural component testing. Computer programs developed to design the bending load frame, and the design process and stress analysis developed herein can be applied to the structural design of other similar testing machines or structures.

Finite element analysis was performed for the structural torsional load frame and it was found adequate for torsional fatigue testing of various shafts or torsion bars.

The application of the structural fatigue testing machine developed can assure product integrity, reliability, and provide unprecedented insights into product performance.

ACKNOWLEDGEMENTS

This research was performed at the Korea Institute of Machinery and Metals and supported by the Ministry of Science and Technology. C. S. Rho, Y.H. Park, W.D.Kim of KIMM contributed to this research at different stages. Professors C.H.Kang and P.H.Chang provided valuable suggestions.

REFERENCES

Boresi,A.P., Sidebottom, O.M., Seely,F.B., and Smith,J.O., 1978, Advanced Mechanics of Materials, John Wiley & Sons, pp. 175~184.

Fuchs, H.O. and Stephens, R.I., 1980, Metal Fatigue in Engineering, John Wiley & Sons, pp. 7~9, 120~122.

Lee, S.B. et al., 1983, Development of a Large Structural Fatigue Testing Machine (I), KIMM Research Report CRN 119~297 C., Korea.

Lee, S.B., 1985, "Structural Fatigue Tests of Automobile Components under Constant Amplitude Loadings," ASM Proc. Fatigue Life Analysis and Prediction, Salt Lake City, pp. 177~186.

Lee, S.B. et al., 1988, Development of Testing Technology for Machine Components(Ⅲ), KIMM Research Report UCN122-1039.C, Korea.

Lee, S.B. and Lee, J.C., 1989, "Vibrational Aspects in Structural Fatigue Testing," Experimental Mechanics, Vol. 29, No.4, pp. 405~408.

Little, R.E. and Ekvall, J.C., 1979, Statistical Analysis of Fatigue Data,ASTM STP 744.

Tse, F.S., Morse, I.E. and Hinkle, R.T., 1978, Mechanical Vibrations Theory and Application, 2nd ed. Allyn & Bacon, INC.

Zandman, F., Redner, S., and Daly, J.W., 1977, Photoelastic Coatings, SESA, Monograph No.3.